Prediction of half reaction length for H₂-O₂-Ar detonation with an extended vibrational nonequilibrium Zel'dovich −von Neumann −Döring (ZND) model

Ken Chunkit Uy, Lisong Shi, Chihyung Wen

Abstract

An extended Zel'dovich–von Neumann–Döring (ZND) model has been proposed to address vibrational nonequilibrium mechanism. To expand the application of this extended ZND model in predicting flow characteristics under thermal nonequilibrium for hydrogen-related detonation simulations, a case of one-dimensional stoichiometric hydrogen-oxygen detonation with argon dilution is adopted for comparative study. A vibrational relaxation timescale is introduced in the extended ZND model together with simplified single-step and two-step chemical reaction models. In addition, a numerical simulation using the conservation element and solution element (CE/SE) algorithm and detailed chemistry with vibrational nonequilibrium coupling is conducted to serve as a benchmark for the model predictions. In this specific case study, predictions of half reaction length are in good agreement with simulations if the single-step Arrhenius model and the characteristic vibrational temperature of hydrogen are used. Compared with the detailed numerical simulations, the current extended ZND model and the simplified chemical models are demonstrated feasible and economical to predict the half reaction thickness under the vibrational nonequilibrium condition and can serve as one of the analytical tools in studying large-scale H₂-O₂ detonation.

Nomenclature

C_v	Heat capacity at constant volume
E	Total specific energy
e	Total specific internal energy
$E_{a,ind}$	Activation energy for induction model
$E_{a,react}$	Activation energy for reaction model
e_v	Specific vibrational energy
k_{ind}	Pre-exponential factor for induction model
k_{react}	Pre-exponential factor for reaction model
$\mathcal{L}_{1/2}$	Half reaction length
$\mathcal{L}_{ind}$	Induction zone length
$\mathcal{L}_{react}$	Reaction zone length
M	Mach number

N	Molar mass of species
p	Pressure
Q	Heat of reaction
R	Specific gas constant
t	Time
T	Temperature
u	Velocity
v	Specific volume
ω_β	Rate change for induction model
ω_λ	Rate change for reaction model
x	Propagation length
X	Molar fraction for the corresponding species
β	Reaction progress variable for induction model
γ	Specific heat ratio
θ	Characteristic vibrational temperature
λ	Reaction progress variable for reaction model (Mass fraction of product)
μ	Reduced mass
ρ	Density
τ_v	Vibrational relaxation time

Superscript

*	Dimensional form

Subscript

avg	Geometric average
eq	Thermal equilibrium state
Neq	Vibrational nonequilibrium state
tr	Translation-rotational mode
v	Vibrational mode
vn	von Neumann state
0	Initial reactant state

Introduction

Numerical studies of detonation have been conducted for many decades. Various applications such as hazardous analyses in coal mine gas explosions, explosion issues

in industry, hydrogen-combustion in nuclear plants and development of pulse detonation engines [1-5] requires fundamental researches on the gas detonation initiation and propagation mechanism. With the emerging high-power computers, multi-dimensional numerical simulations of detonation problems with detailed chemistry models have become feasible. Jiang et al. [6] have made an extensive and excellent review on initialization and propagation of gas detonation wave using computation fluid dynamics (CFD). However, studies have revealed a persistent discrepancy in detonation cell size between numerical simulations and experimental observations. For a stoichiometric argon-diluted hydrogen-oxygen mixture, the simulated cells are approximately half the measured values. Taylor et al. [7] suggested that this discrepancy is due to the neglect of the vibrational relaxation process in high-temperature reactive flows. To explain this disagreement, Shi et al. [8] conducted numerical simulation of argon-diluted H_2-O_2 detonation under four scenarios with both thermal equilibrium and nonequilibrium assumptions and made the comparison, which are (i) the whole system is in thermodynamic equilibrium; (ii) the vibrational relaxation is considered and the translational-rotational temperature is used as the dominant temperature of the chemical reactions; (iii) the same non-equilibrium effect as in the second scenario is used along with Park's two-temperature model [9] to account for the effect of vibrational temperature on chemical reaction rates; and (iv) a more physically consistent coupled-vibration-chemistry-vibration model (CVCV) [10] is adopted. They reported that the disparity in cell width with experimental measurement was greatly narrowed down to a factor of 1.33 and 1.32, respectively, if Park's two-temperature model and the CVCV model were used to include the effects of vibrational relaxation and coupling between molecular vibrations and chemical reactions. As also known from previous studies, the half reaction thickness and detonation cell size are directly related [11]. Therefore, it is clear that the thermal equilibrium assumption in conventional detonation studies needs to be further examined, especially with the consideration of vibrational nonequilibrium.

Despite plentiful numerical simulations and experimental studies concerning fundamental detonation problems, classical theoretical efforts remain the cornerstone of detonation physics [12]. Using Chapman-Jouguet (CJ) theory, detonation wave speed and downstream equilibrium thermodynamic state properties can be obtained for a given initial upstream state. A well-known theoretical model for the detonation propagation process under chemical reactions, the Zel'dovich–von Neumann–Döring (ZND) model, was later introduced in the 1940s [13-15]. The CJ state properties predicted by the ZND model are still widely used to validate numerical simulations. However, this theoretical model is based on the thermodynamic equilibrium assumption. Previous numerical findings on the effects of vibrational relaxation on detonation

suggest that this physical mechanism is of interest to detonation science and should be included in theoretical models such that its importance can be examined.

Tarver was the first one to consider the thermodynamic nonequilibrium in ZND model and the extended theory was named as the nonequilibrium ZND (NEZND) theory [16-18]. In this theory, a detonation wave profile consists of four discrete zones including (1) leading shock front with compressed unreacted mixture; (2) relaxation zone for rotational-vibrational modes of unreacted gases; (3) a thin zone where chemical energy is released by rapid chain propagation and branching reactions; and (4) another relaxation zone for the expansion of product gas towards thermodynamic equilibrium at the CJ state. However, the step-by-step thermal equilibrium assumption may not always be valid and the continuous evolution of the detonation process is missing in the NEZND model. Accordingly, Uy et al. [19] proposed another extended ZND model with continuous profile to manifest the importance of vibrational-chemical coupling effect in the gaseous detonation process. A parametric study was presented with both single-step and two-step Arrhenius models.

Since the analysis from the traditional ZND profile specifies the detonation structure at steady state [12], the results of numerical simulations using Euler equations and the extended ZND model, under either the thermal equilibrium or nonequilibrium conditions, should converge to the ZND solutions at the end of the detonation process. Combining with our earlier numerical approach (Shi et al. [8]), the prediction of the increase of detonation cell size and half reaction thickness using the extended ZND model (Uy et al. [19]) with consideration of the vibrational relaxation becomes possible. The simplicity of the extended ZND model, compared with the computation-costly numerical simulation with detailed chemistry, can serve as one of the analytical tools in studying large-scale H_2-O_2 detonation, and retain the major detonation physics meanwhile.

The objective of this study is three-fold. Firstly, a one-dimensional (1D) numerical simulation of H_2-O_2 detonation diluted in 70% argon is conducted with the consideration of detailed chemical reactions and vibrational relaxation, following the example of Shi et al. [8]. The result of the 1D numerical simulation will serves as a benchmark for the simplified model analyses, where the chemical reaction related vibrational nonequilibrium effect on the ZND model proposed by Uy et al. [19] is applied. Secondly, to imitate and simplify the detailed chemical reactions applied in the numerical simulation, both single-step and two-step Arrhenius models are implemented in the extended ZND model by a fitting process, which has been thoroughly discussed by Taylor et al. [20] in examining the influence of chemical kinetics on hydrogen-air detonations. The extended ZND model is then integrated along the reaction profile with the consideration of the selected vibrational relaxation parameters. Thermodynamic

equilibrium and nonequilibrium cases are presented in terms of half reaction thickness and the resulting profiles are compared with those obtained by the numerical simulations. Thirdly, a 1D numerical simulation is conducted with the fitted single-step and two-step reaction models to justify the appropriateness of integrating the simplified chemical models into the numerical simulation for predicting the half reaction length.

Governing equations for extended ZND model

The detailed derivations of the conventional steady ZND model and the extended ZND model with vibrational nonequilibrium effect considered using Euler equations have been described thoroughly by Fickett and Davis [21] and Uy et al. [19], respectively. For the clarity of the context, the extended ZND model will be introduced briefly as follows.

Because there are four basic internal energy modes for molecules—translational, rotational, vibrational, and electrical [22] , the vibrational relaxation process is considered by separating the internal energy term in the energy equation into two parts (translational-rotational energy mode and vibrational energy mode), assuming both the translational mode and rotational mode reach equilibrium quickly right after the shock and the electrical mode is not excited. Consequently, normalized energy equations are described as: (the superscript * denotes the dimensional quantities)

$$E = e + \frac{u^2}{2} = \frac{p}{\rho(\gamma-1)} - \lambda Q + \frac{u^2}{2} = \frac{\alpha p}{\rho(\gamma-1)} + e_v - \lambda Q + \frac{u^2}{2}, \tag{1}$$

$$e_v^* = \frac{\theta^*}{e^{\theta^*/T_v^*} - 1} R, \; e_v = \frac{e_v^*}{RT_0}, \tag{2}$$

$$\alpha = \frac{C_{v,tr}}{C_{v,tr} + C_{v,v}\dfrac{T_v}{T_{tr}}}, \tag{3}$$

Notably, α is introduced into the formulation to separate out the vibrational energy mode from the internal energy for assessment. It is defined as the ratio of specific heat capacity at constant volume for the translational energy mode versus that for the total energy mode. RT_0 is presented in Eq. (2) for the purpose of normalization as analogous to the formulation discussed in the later paragraph (i.e. Eq (17)). Both $C_{v,tr}$ and $C_{v,v}$ are defined by the degree of freedom of molecules and the temperature derivatives of e_v respectively and are discussed in [19, 22].

The Rankine-Hugoniot relation can then be formulated based on the conservation of mass, momentum, and the modified energy equations discussed above, i.e. Eqs. (1)-(3). Normalized thermodynamic properties across the profile are then reformulated as

follows [19]:

$$\rho = \frac{M^2(\gamma + 1 + 2\varsigma)}{(\gamma M^2 + 1)(1 + \frac{\varsigma}{\gamma})[1 \mp w_\rho(\varsigma)\xi(\lambda, e_v, \varsigma)]} \tag{4}$$

$$p = \frac{(\varsigma + 1)(\gamma M^2 + 1)}{(\gamma + 1 + 2\varsigma)}[1 \pm \gamma w_p(\varsigma)\xi(\lambda, e_v, \varsigma)] \tag{5}$$

$$\varsigma = \alpha - 1 \tag{6}$$

$$w_\rho(\varsigma) = \frac{M^2 - 1}{(\gamma M^2 + 1)(1 + \frac{\varsigma}{\gamma})} \tag{7}$$

$$w_p(\varsigma) = \frac{M^2 - 1}{(\gamma M^2 + 1)(\varsigma + 1)} \tag{8}$$

$$\xi(\lambda, e_v, \varsigma) = (1 - \frac{\lambda q}{\Omega(\varsigma)} + \frac{e_v}{\Omega(\varsigma)} + \frac{\varsigma^2}{\Phi_1} + \frac{\varsigma}{\Phi_2})^{1/2} \tag{9}$$

$$\Omega(\varsigma) = \frac{\gamma(M^2 - 1)^2}{2M^2(\gamma^2 - 1 + 2\varsigma(\gamma - 1))} \tag{10}$$

$$\Phi_1 = \frac{\gamma^2(M^2 - 1)^2}{(\gamma M^2 - 1)^2} \tag{11}$$

$$\Phi_2 = \frac{\gamma(M^2 - 1)^2}{2(\gamma M^4 + 1)} \tag{12}$$

The two solutions with negative and positive signs in Eq. (4) (positive and negative signs in Eq. (5), correspondingly) indicate the strong and weak detonation solutions, respectively; only is the strong detonation solution presented in this paper.

Chemical reaction along the profile can be modelled by a single-step Arrhenius equation or a two-step model. The rate of change of reaction progress variable in single-step model can be described as:

$$\frac{d\lambda}{dt} = k(1 - \lambda)exp\left(-E_a \frac{T_{vn}}{T}\right), \tag{13}$$

On the other hand, considering the detonation driven by chain-branching kinetics, Ng et al. [23] introduced a temperature-sensitive Arrhenius equation to include the thermally neutral induction period before the reaction zone. This induction Arrhenius equation is further combined with the heat release stage described in Eq. (13) and form a two-step model, formulated as follows:

$$\omega_\beta = \frac{d\beta}{dt} = H(1 - \beta) \cdot k_{ind} exp\left[E_{a,ind}\left(1 - \frac{T_{vn}}{T}\right)\right], \tag{14}$$

$$H(1 - \beta)\begin{cases} = 1 \ if \ \beta \ < 1 \\ = 0 \ if \ \beta \ \geq 1 \end{cases}, \tag{15}$$

$$\omega_\lambda = \frac{d\lambda}{dt} = (1 - H(1 - \beta)) \cdot k_{react}(1 - \lambda)e^{-E_{a,react}T_{vn}/T}. \tag{16}$$

The step function $H(1 - \beta)$ in Eqs (14)-(16) ensures that the heat release stage starts only if induction period is ended at $\beta \geq 1$, while β is set to be 0 initially.

Notably, the physical quantities in Eqs. (4) to (16) have been normalized with respect to the state of the unburned reactants (subscript 0) or the von Neumann state (subscript vn) as follows:

$$\rho = \frac{\rho^*}{\rho_0}, p = \frac{p^*}{p_0} = \frac{\rho_0 R T^*}{p_0}, T = \frac{T^*}{T_0}, u = \frac{u^*}{\sqrt{RT_0}}, E = \frac{E^*}{RT_0},$$

$$x = \frac{x^*}{\mathcal{L}_{1/2}}, t = \frac{t^*}{\mathcal{L}_{1/2}/\sqrt{RT_0}}, \tau_v = \frac{\tau_v^*}{\mathcal{L}_{1/2}/\sqrt{RT_0}}, Q = \frac{Q^*}{RT_0},$$

$$k_{ind(react)} = \frac{k_{ind(react)}^*}{\sqrt{RT_0}/\mathcal{L}_{1/2}}, E_{a,ind(react)} = \frac{E_{a,ind(react)}^*}{RT_{vn}} \tag{17}$$

$\mathcal{L}_{1/2}$ is the half reaction thickness, which is defined as the distance from the shock to where one half of the reactant is consumed from the initial state. The von Neumann state properties for the ZND model can be evaluated from the conventional Rankine-Hugoniot relation, with the γ obtained from the 1D numerical result with detailed chemistry.

To demonstrate the vibrational-chemical coupling effect in the simplest fashion, Park's two temperature model [9] is used, and T in Eqs. (13)-(16) is replaced by the average temperature T_{avg}, defined as

$$T_{avg} = (T_{tr}T_v)^{1/2}. \tag{18}$$

To evaluate the energy transfer rate between the translational-rotational mode and the vibrational mode, ω_v, the Landau-Teller model is applied:

$$\omega_v = \frac{e_v^{eq} - e_v}{\tau_v}, \tag{19}$$

where e_v^{eq} is the vibrational energy under thermal equilibrium, i.e. when $T_v = T_{tr}$. An

empirical model formulated by Millikan and White [24] is commonly used to estimate vibrational relaxation time τ_v^* and is summarized below:

$$\tau_{v,i-j}^* = \frac{1}{p^*} exp\left[A\left(T^{*-\frac{1}{3}} - B\right) - 18.42\right], \tag{20}$$

$$A = 0.00116\mu^{1/2}\theta^{*4/3}, B = 0.015\mu^{1/4}, \tag{21}$$

$$\mu = \frac{N_i N_j}{N_i + N_j}, \tag{22}$$

μ is defined when primary species i interacts with species j through molecular collisions. This model also requires the input of corresponding p^*, T^*, and θ^* for primary species i across the profile. The vibrational relaxation time of species i in a mixture of different gases, i.e. species i (self-interaction), j and k can be determined by the following equation:

$$\frac{1}{\tau_{v,i}^*} = \frac{X_i}{\tau_{v,i-i}^*} + \frac{X_j}{\tau_{v,i-j}^*} + \frac{X_k}{\tau_{v,i-k}^*}, \tag{23}$$

where X is the molar fraction for the corresponding species interacting with primary species i, and $\tau_{v,i-i}$, $\tau_{v,i-j}$ and $\tau_{v,i-k}$ are the vibrational relaxation time of species i infinitely dilute in species i (self-interaction), k, and l, respectively [25]. Corresponding τ_v^* can then be obtained through the summation. In this paper, τ_v^* is estimated by both the primary reactants H_2 and O_2, with their corresponding species interactions, i.e. H_2-H_2, H_2-O_2, H_2-Ar and O_2-H_2, O_2-O_2, O_2-Ar, respectively. The mass fraction of the species H_2:O_2:Ar are set to be 2:1:7 (same as the initial reactant mass fractions in the numerical simulation). Noted that $\mathcal{L}_{1/2}$ is required to normalize τ_v^* (see Eq. (17)) and is obtained through the analysis of corresponding numerical cases under the thermal equilibrium assumption.

$\xi(\lambda, e_v, \varsigma)$ in Eqs. (4) and (5) represents the chemical and vibrational coupling relation in the extended ZND profile. Its value range is between 1 (product state) and 0 (reactant state), and $\alpha < 1$ is always valid across the profile if the vibrational relaxation process is presented. Notably, the results of the extended ZND model will later be compared with those of 1D numerical simulation of H_2-O_2-Ar detonation with

detailed chemistry.

Numerical method for simulation

The structure of 1-D detonation can be determined by solving the unsteady Euler equations,

$$\frac{\partial \boldsymbol{U}}{\partial t} + \frac{\partial \boldsymbol{F}}{\partial x} = \boldsymbol{S}, \tag{24}$$

where $\boldsymbol{U}$, $\boldsymbol{F}$, and $\boldsymbol{S}$ are the conserved variables, corresponding fluxes, and source terms, respectively. Applying the detail chemistry model, the above variables are described as follows

$$\boldsymbol{U} = [\rho_i, \rho u, \rho E, \rho e_v], \tag{25}$$
$$\boldsymbol{F} = [\rho_i u, \rho u^2 + p, (\rho E + p)u, \rho e_v u], \tag{26}$$
$$\boldsymbol{S} = [\rho_i \omega_i, 0, 0, \rho \omega_v], \tag{27}$$

where ω_i is the rate change caused by chemical reactions. If a single-step or a two-step model is used instead, the variables are formulated accordingly as:

$$\boldsymbol{U} = [\rho, \rho u, \rho E, \rho e_v, \rho \lambda, \rho \beta], \tag{28}$$
$$\boldsymbol{F} = [\rho u, \rho u^2 + p, (\rho E + p)u, \rho e_v u, \rho \lambda u, \rho \beta u], \tag{29}$$
$$\boldsymbol{S} = [0, 0, 0, \rho \omega_v, \rho \omega_\lambda, \rho \omega_\beta], \tag{30}$$

where β is set to 0 initially for the two-step model and is set to be unity initially for single-step model.

In this study, a conservation element and solution element (CE/SE) method [8] of second-order accuracy based on uniform meshes is implemented to solve the multi-species Euler equations coupled with simplified/detailed chemical mechanisms and vibrational energy relaxation. The CE/SE method, originally proposed by Chang et al. in the 1990s [26], unifies the treatment of space and time and is capable of capturing the shock structure without using Riemann solvers. The compactness of the scheme makes it ideal for parallel computing. Since its inception, the CE/SE method has been successfully utilized in the computation of hypersonic reentry flows [27, 28], detonation waves [8, 29], and compressible multiphase problems [30-32].

To fully resolve the stiff source term, a fractional step-splitting method is used, in which the calculation of transport and the integration of reactions are performed separately. A detailed chemistry model for high-pressure and high-temperature

hydrogen combustion by Burke et al. [33] is used in the simulations. This mechanism involves 25 elementary reactions among 9 species. To characterize the effect of vibrational non-equilibrium on reaction rates, the forward Arrhenius reaction rate is described as a function of geometrically averaged temperature (Park's two-temperature model [9]). A mesh size of 5 μm is used for all simulations in this study, as further refinement do not change the structure of the detonation in the simulation [8].

Result and discussion

For purposes of comparison with the numerical results under vibrational non-equilibrium assumption, data obtained from the 1D CE/SE simulations with detailed chemistry under thermal equilibrium conditions are first used to determine the parameters in both single-step Arrhenius equation and two-step chain branching kinetics in the extended ZND model. Hydrogen-oxygen detonation with 70% Argon dilution under initial temperature of 300K is the selected case for investigation, in which the role of vibrational nonequilibrium effect has been discussed by Shi et al. [8] before. We aim at finding a simplified chemical/vibrational kinetics such that the half reaction length predicted can be as close to that in numerical simulation, while retaining the fundamental detonation physics in the meantime. Finally, the selected simplified model is then implemented in 1D numerical simulation for justification.

Modified single-step & two-step Arrhenius model to fit with detail chemistry model
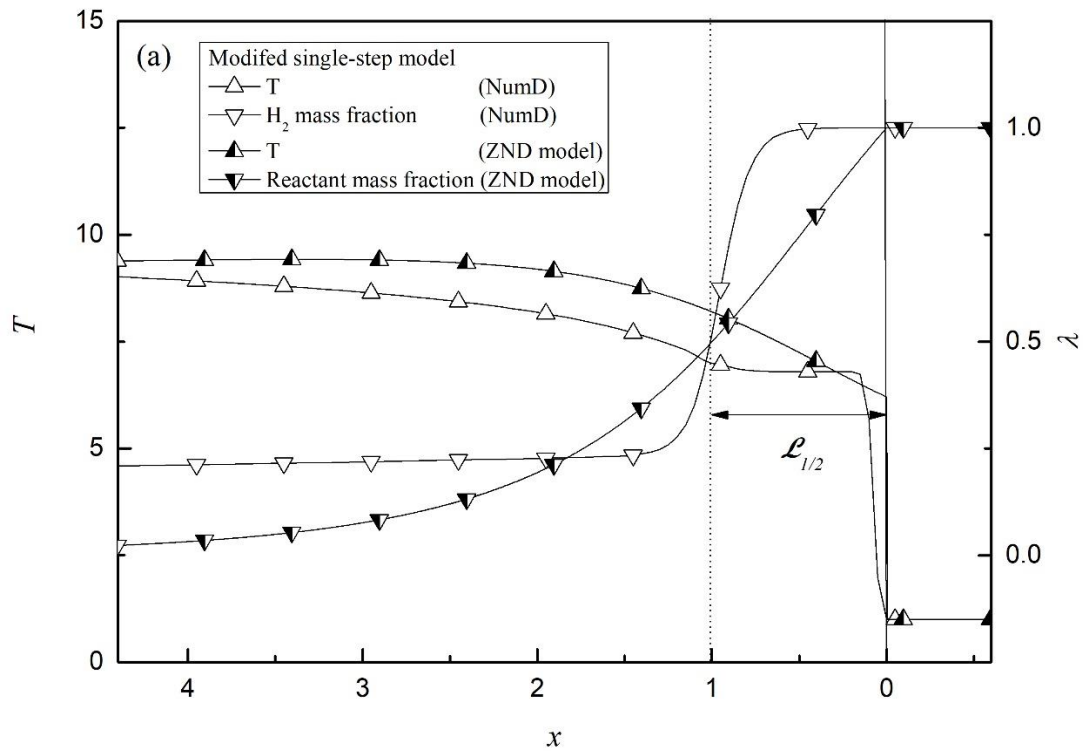
The extended ZND model with both modified single-step and two-step models were integrated along the reaction profile with initial pressure set as 0.1, 0.2, 0.3, and 0.4 atm respectively. Following the approach by Taylor et al. [20], the parameters in the single-step model (i.e. Eq. (13)) was reduced by a fitting process to the detailed chemistry model. In their discussion, Q and γ in the single-step model were fixed to match the CJ detonation velocity (and hence the same CJ Mach number M_{CJ}) and then k was adjusted with several choices of E_a to get the desired half reaction thickness $\mathcal{L}_{1/2}$. The choice of E_a followed the analysis of the thermodynamic data recently developed by Burke et al. [33] which has also been adopted by Shi et al. [8] and Taylor et al. [7], while the values of M_{CJ} and γ (on the product side) were taken from the results computed by Shi et al. [8] under the thermal equilibrium state. Q was evaluated from the relation $M_{CJ} = (2(\gamma^2 - 1)Q)^{1/2}$.

Considering the two-step chain-branching kinetics in Eqs. (14)-(16), the approach of Ng et al. [23] was adopted where $E_{a,ind}$ and $E_{a,react}$ were set to be 4 and 1, respectively, for the H2-O2 mixture in all initial pressure cases to ensure that $E_{a,ind} \gg E_{a,react}$. Values of γ and Q were shared by the cases in the modified single-step model. The ratio of induction zone length $\mathcal{L}_{ind}$ to reaction zone length $\mathcal{L}_{react}$

was set to be 1:1, according to the numerical simulation results of Shi et al. [3]. Here, the reaction zone length $\mathcal{L}_{react}$ is defined as the zone starts from the end of induction zone to where half of the reactant is consumed. A summary of the parameters is listed in Table 1. Thermodynamic properties in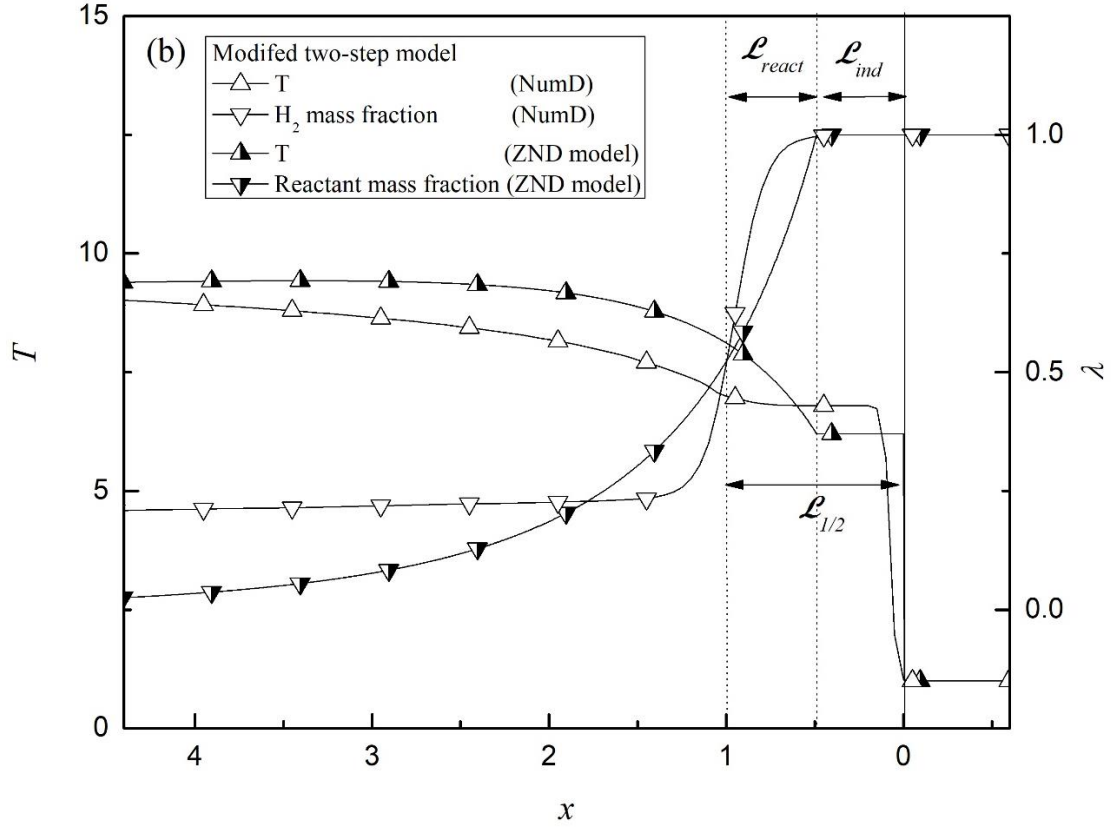 von Neumann state were evaluated using Rankine-Hugoniot relation. Figure 1 shows the normalized temperature and reactant mass fraction profiles at the thermal equilibrium state using (a) the modified single-step and (b) the two-step models, compared with those by CE/SE simulations using the detailed chemistry model. Over 200 mesh points were used per half reaction thickness for integration across the ZND profile. It is expected that the two-step model shows a better fitting to the numerical simulation than the single-step counterpart and the induction zone $\mathcal{L}_{ind}$ can be manifested clearly. Although this zone is absent in the modified single-step model, the fairly similar trend is still observed.

Table 1 – Normalized parameters analyzed by the data of 1D CE/SE simulation with the chemical kinetic model of Burke et al. [33].

Initial Pressure (atm)	γ (product side)	Q	E_a (Single-step model)
0.1	1.45	11.9	4.2
0.2	1.44	13.7	4.4
0.3	1.44	15.0	4.4
0.4	1.44	15.3	4.4

Fig. 1. Comparison of normalized temperature T and reactant mass fraction λ profiles at the thermal equilibrium state using (a) the modified single-step model (b) the two-step model in the extended ZND model, with the numerical simulation results (NumD) using detailed chemistry model. Shock wave is encountered at normalized $x = 0$ (Eq. (17)) and propagates from left to right.

Comparison of half reaction length ratio estimated from the extended ZND model with numerical simulation

Up to now, the only initial parameter that remains to be determined for the prediction of the half reaction length under vibrational nonequilibrium condition is the characteristic vibrational temperature θ^*. Unlike the 1D numerical simulation with a detailed chemistry model, in which all possible species in the reaction are considered, the extended ZND model only involves a single species. Therefore, in this study, either reactant H_2 or O_2 is adopted as the major species in the model for simplification and for purposes of comparison with the 1D CE/SE benchmark simulations. The two choices of reactant in the simplified model is manifested in terms of the characteristic vibrational temperature θ^* (i.e. $\theta_{O2}^* = 2250\ K$ or $\theta_{H2}^* = 5989\ K$ as referenced from [34]). Four scenarios with vibrational nonequilibrium assumption were conducted in each initial pressure case as listed below.

Case (i): $\theta_{H2}{}^*$ is adopted using the modified single-step model.

Case (ii): $\theta_{H2}{}^*$ is adopted using the modified two-step model.

Case (iii): $\theta_{O2}{}^*$ is adopted using the modified single step model.

Case (iv): $\theta_{O2}{}^*$ is adopted using the modified two-step model.

The 1D numerical simulations with thermal equilibrium and nonequilibrium assumptions in each initial pressure case are served as the baselines for comparison.

Figure. 2 shows the half reaction length ratios calculated from both the equilibrium and the nonequilibrium numerical simulations and from the extended ZND model with different characteristic vibrational temperature θ^* under a range of initial pressure. The half reaction length ratio, $\mathcal{L}_{1/2}$ ratio, is defined as the ratio of the half reaction length at the vibrational nonequilibrium state (*Neq*) to the half reaction length at the vibrational equilibrium state (*eq*). Notably, $\mathcal{L}_{1/2}$ ratio = 1 for the equilibrium simulation (show as the dashed line in Fig. 2) is for the comparison of different nonequilibrium predictions. From the vibrational nonequilibrium simulation results, although the exact half reaction lengths in different initial pressure cases are not the same (as shown in Shi et al.'s work [8]), the normalized half reaction length ratio show small variations among different initial pressures. The prediction from the extended ZND model shows an elongation of half reaction length under the vibrational nonequilibrium assumption in every case, no matter $\theta_{H2}{}^*$ or $\theta_{O2}{}^*$ is used. Their growth trends of $\mathcal{L}_{1/2}$ ratio are similar with that of the vibrational nonequilibrium simulations. It implies that no matter what chemical kinetics is selected, the vibrational nonequilibrium effect is crucial in the H_2-O_2 detonation and can be always manifested even in simplified models in terms of the half reaction thickness. These observations agree with the conclusion discussed by Shi et al. [8] and Uy et al. [19]. The vibrational relaxation process slows down the chemical reaction rate across the profile, which can be explained by the inter-transfer mechanism of translational-rotational energy to vibrational energy. The average temperature $T_{avg,Neq}$ (denoted in Eq. (18)) therefore is always lower than T_{eq} as modelled by Park's two-temperature model, and so does the chemical rate (manifested in terms of zone thickness).

On the other hand, as shown in Fig. 2, better agreement with the 1D numerical result is observed if $\theta_{H2}{}^*$ is used for prediction than $\theta_{O2}{}^*$. The accuracy of prediction by using $\theta_{H2}{}^*$ in the single-step model and the two step model ranges approximately from 1% to 11% and from 3% to 7%, respectively, whereas that by $\theta_{O2}{}^*$ ranges approximately from 14% to 20% and from 18% to 20%, respectively (also see Table 2). The closer prediction in using $\theta_{H2}{}^*$ implies that H_2 might be a dominant reactant in vibrational relaxation mechanism for this reaction process. Similar computation results have been discussed by Taylor et al.'s analysis [25] on estimating the vibrational

nonequilibrium time scale in hydrogen-air detonation, in which they showed H_2 vibrational relaxation time is much longer than that of O_2, indicating the dominant role of H_2 in the vibrational nonequilibrium process. Notably, regarding the natures of the selected models, the two-step model introduces more variables and in other words, its degree of freedom in much larger than that in the single-step model. Therefore, the choice of parameters must be more critical in order to have better predictions for the two Arrhenius equations representing the two zones.
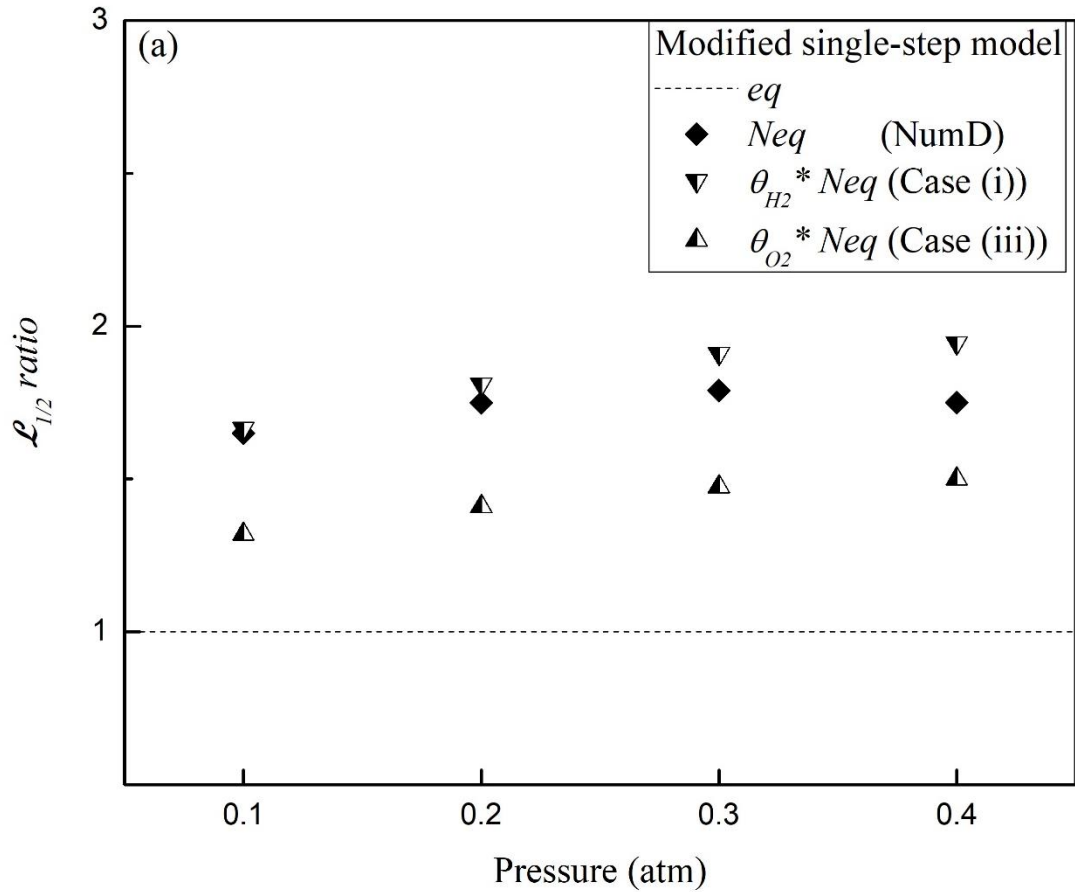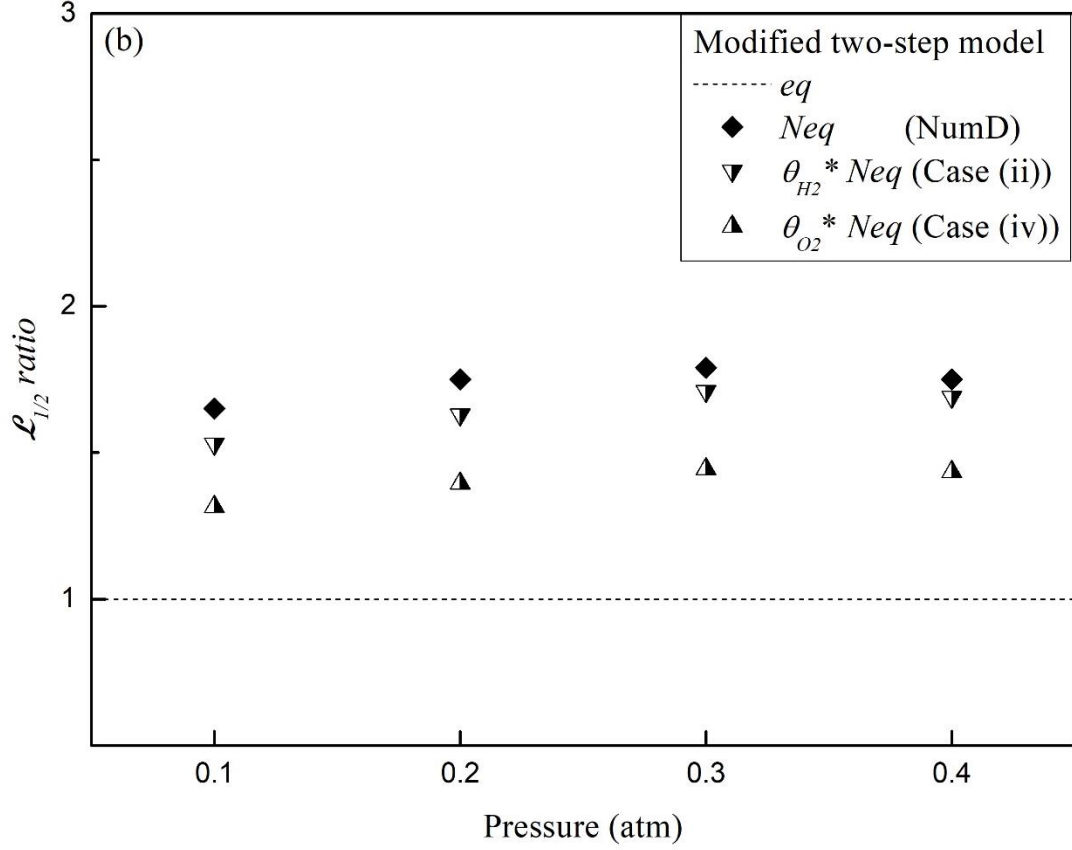
Fig. 2. Half reaction length ratio versus initial pressure when considering (a) modified single-step model (b) modified two-step model in the extended ZND model with the reactant H_2 as the major species under the *Neq* state (Case (i) & Case (ii)) and the reactant O_2 as the major species under the *Neq* state (Case (iii) & Case (iv)). The results of 1D numerical simulations with the detail chemistry model (NumD) under vibrational equilibrium state (*eq*) and vibrational nonequilibrium state (*Neq*) are also shown for comparison.

Implementation of the simplified chemical models into the 1D numerical simulation

To justify the appropriateness of using the simplified single-step/two-step models in predicting the half reaction thickness, 1D CE/SE numerical simulations were further conducted using these simplified chemical models with θ_{H2}^* for the chemical-vibrational coupling, instead of the detail chemistry model by Burke et al. [33]. Notably, adopting θ_{H2}^* in the extended ZND model yields a better prediction of the half reaction thickness than θ_{O2}^*, as discussed above. The solution was converged if 40 points per half reaction length of the steady ZND solution were used. Summary of cases with different initial pressure and different chemical models are presented in Table 2. The difference in the $\mathcal{L}_{1/2}$ ratio between the predicted solutions (ZND) and the simulated solutions with simplified single-step and two-step chemical models (NumS)

has the difference (%diff) at most of 16% with the simulations with detail chemistry model (NumD). The appropriateness of using the simplified single-step/two-step models in the CFD simulations for prediction of the half reaction thickness is justified.

Table 2. Comparison of normalized half reaction length using selected chemical models					
Pressure (atm)	$\mathcal{L}_{1/2}$ ratio at *Neq* state				
	NumD	Case (i) (θ_{H2}^*, Single-step)		Case (ii) (θ_{H2}^*, Two-step)	
		ZND (%diff)	NumS (%diff)	ZND (%diff)	NumS (%diff)
0.4	1.75	1.95 (11.4%)	2.03 (16.0%)	1.69 (3.4%)	1.71 (2.3%)
0.3	1.79	1.91 (6.7%)	2.01 (12.3%)	1.71 (4.5%)	1.75 (2.2%)
0.2	1.75	1.81 (3.4%)	1.92 (9.7%)	1.63 (6.9%)	1.59 (9.1%)
0.1	1.65	1.67 (1.2%)	1.75 (6.1%)	1.53 (7.3%)	1.50 (9.1%)

Note: ZND = from extended ZND model;
NumS = from numerical simulation with simplified chemistry;
NumD = from numerical simulation with detailed chemistry;
%diff = |[(ZND or NumS)-NumD]/NumD x 100%|

Practical implications of the present study

Conventionally, it is known that ZND model is an ideal steady state solution for the Euler simulations. The present work demonstrates that the extended ZND model with the consideration of vibrational nonequilibrium effect is also analytically comparable with the steady state solution of simulations under the same nonequilibrium assumption. Compared with the detailed numerical simulations, the current extended ZND model and the simplified chemical models are much more economical to predict the half reaction thickness and accordingly the detonation cell size in large scale H_2-O_2 detonation simulations under the vibrational nonequilibrium condition, while physics in chemical-vibrational coupling mechanisms mostly retained.

Conclusion

An extended ZND model with the consideration of chemical-vibrational coupling effect was applied in this paper to predict the half reaction lengths of stoichiometric H_2-O_2-Ar detonation under different initial pressures. Adopting θ_{H2}^* or θ_{O2}^* in the extended ZND model along with the modified single-step and two-step chemical

models, four scenarios under different initial pressures were designed for model prediction. Overall, the matching of the prediction from extended ZND model with single/two-step chemistry and that from numerical simulation are satisfactory. The prediction accuracy of half reaction length compared with the benchmark value by using θ_{H2}^* in the single-step model and the two step model ranges approximately from 1% to 11% and from 3% to 7%, respectively, whereas that by θ_{O2}^* ranges approximately from 14% to 20% and from 18% to 20%, respectively. The better predictions by using θ_{H2}^* (i.e. H_2 as the reactant species) compared with those using θ_{O2}^* indicate that H_2 is a dominant species in the vibrational relaxation mechanism for this particular case of H_2-O_2-Ar detonation. To further justify whether the simplified chemical models are applicable in unsteady Euler numerical simulations, one-dimensional CE/SE simulations implemented with the modified single-step and two-step chemical models were performed and the computed half reaction lengths were compared with the results estimated by the extended ZND model and the simulations using the detail chemistry model under the same nonequilibrium assumption. Small discrepancies were observed. Summarily, the extended ZND model is justified and can be treated as an analytical tool to predict the half reaction length and accordingly the detonation cell size in large scale H_2-O_2 detonation simulations under thermal nonequilibrium assumption, while physics in chemical-vibrational coupling mechanisms mostly conserved.

Reference

[1] Ng HD, Ju Y, Lee JHS. Assessment of detonation hazards in high-pressure hydrogen storage from chemical sensitivity analysis. International Journal of Hydrogen Energy. 2007;32:93-9.

[2] Petukhov VA, Naboko IM, Fortov VE. Explosion hazard of hydrogen–air mixtures in the large volumes. International Journal of Hydrogen Energy. 2009;34:5924-31.

[3] Soury H, Mazaheri K. Utilizing unsteady curved detonation analysis and detailed kinetics to study the direct initiation of detonation in H2–O2 and H2–Air mixtures. International Journal of Hydrogen Energy. 2009;34:9847-56.

[4] Kuznetsov M, Yanez J, Grune J, Friedrich A, Jordan T. Hydrogen combustion in a flat semi-confined layer with respect to the Fukushima Daiichi accident. Nuclear Engineering and Design. 2015;286:36-48.

[5] Smirnov NN, Nikitin VF. Modeling and simulation of hydrogen combustion in engines. International Journal of Hydrogen Energy. 2014;39:1122-36.

[6] Jiang ZL, Teng HH. Research on some fundamental key problems of regular gaseous detonation initiation and propagation under the uniformed frame. SCIENTIA SINICA Physica, Mechanica & Astronomica. 2012;42(2):1-15.

[7] Taylor B, Kessler D, Gamezo V, Oran E. Numerical simulations of hydrogen detonations with detailed chemical kinetics. Proceedings of the combustion Institute. 2013;34:2009-16.

[8] Shi L, Shen H, Zhang P, Zhang D, Wen C. Assessment of Vibrational Non-Equilibrium Effect on Detonation Cell Size. Combustion Science and Technology. 2016;189:841-53.

[9] Park C. Assessment of two-temperature kinetic model for ionizing air. Journal of Thermophysics and Heat Transfer. 1989;3:233-44.

[10] Knab O, Fruehauf HH, Messerschmid EW. Theory and validation of the physically consistent coupled vibration-chemistry-vibration model. Journal of Thermophysics and Heat Transfer. 1995;9:219-26.

[11] Gavrikov A, Efimenko A, Dorofeev S. A model for detonation cell size prediction from chemical kinetics. Combustion and flame. 2000;120:19-33.

[12] Lee JH. The detonation phenomenon: Cambridge University Press Cambridge; 2008.

[13] Zeldovich YB. On the theory of the propagation of detonation in gaseous systems. 1950.

[14] Von Neumann J. Theory of detonation waves. O.S.R.D. Rept.; 1942. p. 549.

[15] Döring W. Über den Detonationsvorgang in Gasen [On detonation processes in gases]. Annalen der Physik. 1943;43:421-36.

[16] Tarver CM. Chemical energy release in one-dimensional detonation waves in gaseous explosives. Combustion and Flame. 1982;46:111-33.

[17] Tarver CM. Chemical energy release in the cellular structure of gaseous detonation waves. Combustion and Flame. 1982;46:135-56.

[18] Tarver CM. Chemical energy release in self-sustaining detonation waves in condensed explosives. Combustion and Flame. 1982;46:157-76.

[19] Uy KC, Shi L, Wen CY. Chemical reaction mechanism related vibrational nonequilibrium effect on the Zel'dovich−von Neumann−Döring (ZND) detonation model. Combustion and Flame. 2018;196:174-81.

[20] Taylor B, Kessler D, Gamezo V, Oran E. The Influence of Chemical Kinetics on the Structure of Hydrogen-Air Detonations. 50th AIAA Aerospace Sciences Meeting including the New Horizons Forum and Aerospace Exposition: American Institute of Aeronautics and Astronautics; 2012.

[21] Fickett W, Davis WC. Detonation: University of California Press; 1979.

[22] Vincenti WG, Kruger CH. Introduction to physical gas dynamics1965.

[23] Ng HD, Radulescu MI, Higgins AJ, Nikiforakis N, Lee JHS. Numerical investigation of the instability for one-dimensional Chapman–Jouguet detonations with chain-branching kinetics. Combustion Theory and Modelling. 2005;9:385-401.

[24] Millikan RC, White DR. Systematics of vibrational relaxation. The Journal of chemical physics. 1963;39:3209-13.

[25] Taylor B, Kessler D, Oran E. Estimates of Vibrational Nonequilibrium Time Scales in Hydrogen-Air Detonation Waves. 24th International Colloquium on the Dynamics of Explosive and Reactive Systems, Taipei, Taiwan, July2013.

[26] Chang S-C. The method of space-time conservation element and solution element—a new approach for solving the Navier-Stokes and Euler equations. Journal of Computational Physics. 1995;119:295-324.

[27] Wen CY, Saldivar Massimi H, Shen H. Extension of CE/SE method to non-equilibrium dissociating flows. Journal of Computational Physics. 2018;356:240-60.

[28] Shen H, Wen C-Y. Theoretical investigation of shock stand-off distance for non-equilibrium flows over spheres. Chinese Journal of Aeronautics. 2018;31:990-6.

[29] Shen H, Liu K-X, Zhang D-L. Three-Dimensional Simulation of Detonation Propagation in a Rectangular Duct by an Improved CE/SE Scheme. Chinese Physics Letters. 2011;28:124705.

[30] Shen H, Wen C-Y, Parsani M, Shu C-W. Maximum-principle-satisfying space-time conservation element and solution element scheme applied to compressible multifluids. Journal of Computational Physics. 2017;330:668-92.

[31] Shen H, Wen C-Y, Zhang D-L. A characteristic space–time conservation element and solution element method for conservation laws. Journal of Computational Physics. 2015;288:101-18.

[32] Shen H, Wen C-Y. A characteristic space–time conservation element and solution element method for conservation laws II. Multidimensional extension. Journal of Computational Physics. 2016;305:775-92.

[33] Burke MP, Chaos M, Ju Y, Dryer FL, Klippenstein SJ. Comprehensive H2/O2 kinetic model for high-pressure combustion. International Journal of Chemical Kinetics. 2012;44:444-74.

[34] Skrebkov OV. Vibrational non-equilibrium in the hydrogen–oxygen reaction. Comparison with experiment. Combustion Theory and Modelling. 2015;19:131-58.